

Electronic Coherences in Molecules: The Projected Nuclear Quantum Momentum as Hidden Agent

Evaristo Villaseco Arribas and Neepa T. Maitra

Department of Physics, Rutgers University, Newark 07102, New Jersey USA

(Dated: November 13, 2024)

Electronic coherences are key to understanding and controlling photo-induced molecular transformations. We identify a crucial quantum-mechanical feature of electron-nuclear correlation, the projected nuclear quantum momenta, essential to capture the correct coherence behavior. For simulations, we show that, unlike traditional trajectory-based schemes, exact-factorization-based methods approximate these correlation terms, and correctly capture electronic coherences in a range of situations, including their spatial dependence, an important aspect that influences subsequent electron dynamics and that is becoming accessible in more experiments.

Quantum electronic coherences are key factors influencing many photo-induced molecular processes. They serve as control knobs in chemical transformations [1–6] and possibly impact photosynthetic energy flow in biomolecules [7, 8], as well as quantum information science processes [9]. Aside from the practical interest in creating desired products, studying the generation and evolution of coherences, including decay and revival, reveals fundamental properties of how correlations between electrons as well as their interplay with nuclei affect dynamics.

Electronic coherences are usually defined in the Born-Oppenheimer (BO) representation, but nevertheless can be extracted from experiment for the physical reason that away from regions of strong non-adiabatic coupling (NAC), components of the nuclear wavefunction on different BO surfaces evolve independently. The spatially-resolved coherence is defined as [3, 6, 10]

$$\Gamma_{jk}(\underline{\mathbf{R}}, t) = \chi_j^*(\underline{\mathbf{R}}, t)\chi_k(\underline{\mathbf{R}}, t) \quad (1)$$

for $j \neq k$ (and populations $j = k$), where the $\chi_j(\underline{\mathbf{R}}, t)$ are projected nuclear wavefunctions defined via expanding the molecular wavefunction in the BO basis: $\Psi(\underline{\mathbf{R}}, \underline{\mathbf{r}}, t) = \sum_j \chi_j(\underline{\mathbf{R}}, t)\Phi_{\underline{\mathbf{R}},j}(\underline{\mathbf{r}})$, with $\Phi_{\underline{\mathbf{R}},j}$ eigenstates of the BO Hamiltonian $H_{\text{BO}}|\Phi_{\underline{\mathbf{R}},j}\rangle = E_j^{\text{BO}}|\Phi_{\underline{\mathbf{R}},j}\rangle$, where variables $\underline{\mathbf{r}}$, $\underline{\mathbf{R}}$ denote all electronic and nuclear coordinates, respectively. While recent advances in experimental techniques can measure the electronic coherences with sub-Å spatial resolution [2, 3, 11, 12], most experiments instead measure the spatially-averaged coherence [1–6], $\Gamma_{jk}(t) = \int d\underline{\mathbf{R}}\Gamma_{jk}(\underline{\mathbf{R}}, t)$, often referred to as coherence *tout court*.

The electronic coherence thus measures the overlap of the projected wavefunctions. Semiclassical considerations have identified three mechanisms for how this evolves in time, in particular for decoherence (i.e. its decay) [13]: nuclear density overlap decay, pure dephasing, and electronic state transitions. But open questions remain in the nature of the electron-nuclear correlation in influencing coherences, decoherences, and recoherences (i.e. revivals after decoherence): The semi-

classical analyses focus on the spatially-averaged coherence and hold under some assumed wavepacket form and behavior in certain limits [14], so then do these three mechanisms provide a complete picture fully accounting for correlated electron-nuclear dynamics, or do other factors play a key role? While the three mechanisms, and their interplay, have been identified in quantum dynamical simulations [6], how do they explicitly appear in the equations of motion? Computational challenges in modeling complex molecules mean that mixed quantum-classical (MQC) methods are mostly used, where one propagates an ensemble of classical nuclear trajectories each carrying a set of quantum electronic coefficients determined self-consistently through a prescribed quantum-classical feedback; can we precisely identify which quantum properties of the nuclear system influence the evolution of electronic coherence and need to be approximated in such approaches? The most commonly-used methods, Ehrenfest and surface-hopping [15, 16] are both fundamentally unable to correctly capture coherence, with overcoherence in Ehrenfest and internal inconsistency in surface-hopping [15, 17–19]. Ref. [20] pointed out that the commonly-used, largely *ad hoc*, decoherence corrections are fundamentally flawed since they act in a state-wise manner while coherence is a state pair-wise property. Further, if an experiment cannot resolve the spatial character in Eq. 1, an inherent signature of correlation, does it matter if the MQC method does not capture it well if it captures the spatial-average well?

Here we show that even when only the spatially-averaged coherence is measured, the underlying spatial-dependence strongly influences the time-dependence (beyond pure dephasing), and that the projected nuclear quantum momenta, $\nabla_\nu|\chi_j|/|\chi_j|$, are key to capture the correct behavior. Thus electron-nuclear correlation terms that go beyond the earlier semiclassical analyses are essential. Even in cases where traditional trajectory-based MQC simulations yield the correct coherence over the duration of one interaction event, their wrong spatially-resolved coherence leads to poor behavior at

later times. Instead, methods based on the exact factorization (EF) approach [21–25] better approximate these terms and therefore the spatial structure, giving greatly improved predictions, distinguishing between coherence of wavefunctions on parallel surfaces (unlike *ad hoc* decoherence-corrected methods) and gradual decoherence of non-parallel ones (unlike Ehrenfest). While existing EF-based approximations contain a crucial dependence on the overall nuclear quantum momentum, we identify their neglect of the individually projected quantities as the culprit for not accurately capturing decoherence events in regions of negligible NAC.

Coherences evolve due to population transitions from NACs ($\langle \Phi_{\underline{\mathbf{R}},j} | \nabla_{\nu} \Phi_{\underline{\mathbf{R}},k} \rangle$ and $\langle \Phi_{\underline{\mathbf{R}},j} | \nabla_{\nu}^2 \Phi_{\underline{\mathbf{R}},k} \rangle$), but also away from those regions when more than one BO surface is populated. To avoid conflating effects from NACs, we begin by considering the exact equation of motion for the spatially-resolved coherence in a situation where all NACs are zero:

$$i\partial_t \Gamma_{jk}(\underline{\mathbf{R}}, t) = \Delta E_{kj}(\underline{\mathbf{R}}) \Gamma_{jk}(\underline{\mathbf{R}}, t) + \sum_{\nu} \frac{1}{2M_{\nu}} \left(\chi_k(\underline{\mathbf{R}}, t) \nabla_{\nu}^2 \chi_j^*(\underline{\mathbf{R}}, t) - \chi_j^*(\underline{\mathbf{R}}, t) \nabla_{\nu}^2 \chi_k(\underline{\mathbf{R}}, t) \right) \quad (2)$$

where $\Delta E_{kj}(\underline{\mathbf{R}}) = E_k^{\text{BO}}(\underline{\mathbf{R}}) - E_j^{\text{BO}}(\underline{\mathbf{R}})$ and the sum over ν is a sum over all nuclei. Eq. (S.8) in the SM gives the equation including the NACs. Atomic units ($\hbar = m_e = e^2 = 1$) are used throughout this article. The first term on the right of Eq. 2 can be absorbed in a phase, while the evolution of the coherence magnitude depends on the instantaneous curvatures of the BO projected wavefunctions. Instead, when integrated over space, the explicit dependence on these curvatures vanishes, and we find

$$i\partial_t \Gamma_{jk}(t) = \int \Delta E_{kj}(\underline{\mathbf{R}}) \Gamma_{kj}(\underline{\mathbf{R}}, t) d\underline{\mathbf{R}}, \quad (3)$$

that is, the spatially-averaged coherence explicitly depends on the instantaneous relative difference in shape of the BO surfaces weighted by the spatially-resolved coherence. We make two key observations from Eqs. 2–3: First, *without correct spatial dependence of the coherence (a dependence that inherently signifies electron-nuclear correlation), the time-evolution of the spatially-averaged coherence or populations will be wrong.* Second, *for parallel surfaces (no pure dephasing) the magnitude of the spatially-averaged coherence is constant* ($\Gamma_{jk}(t) = e^{i(E_k - E_j)t} \Gamma_{jk}(0)$), *but there is a spatial structure to these quantities that does evolve in time (last two terms of Eq. (2)).*

A deeper understanding of how nuclear motion influences coherences requires to discern local electron-nuclear correlation effects arising from a classical-like treatment of the nuclear motion via an ensemble of trajectories from non-local effects from nuclear wavepacket delocalization. To address this, we turn to the EF,

which, unlike Ehrenfest and surface-hopping, allows a formulation of trajectory-based equations defining exact unique forces on the nuclear trajectories when they are treated classically [26–28], and evolution equations for the populations and coherences. In EF, the molecular wavefunction is represented by a single correlated product, $\Psi(\underline{\mathbf{r}}, \underline{\mathbf{R}}, t) = \chi(\underline{\mathbf{R}}, t) \Phi_{\underline{\mathbf{R}}}(\underline{\mathbf{r}}, t)$ with $\int |\Phi_{\underline{\mathbf{R}}}(\underline{\mathbf{r}}, t)|^2 d\underline{\mathbf{r}} = 1 \forall \underline{\mathbf{R}}, t$ [29–38]. (See also Supplementary Material (SM) for brief details from these works [39]). The EF yields the notion of a unique nuclear wavefunction that satisfies a Hamiltonian evolution and whose modulus and phase give the exact nuclear density and nuclear current-density, $\mathbf{J}_{\nu}(\underline{\mathbf{R}}, t)$, of the molecular wavefunction [35, 36], central concepts to set up an exact trajectory-based approach.

Writing the EF nuclear wavefunction in terms of an amplitude and phase, $\chi(\underline{\mathbf{R}}, t) = e^{iS(\underline{\mathbf{R}}, t)} |\chi(\underline{\mathbf{R}}, t)|$, and likewise for the projected BO wavefunctions, $\chi_k(\underline{\mathbf{R}}, t) = |\chi_k(\underline{\mathbf{R}}, t)| e^{iS_k(\underline{\mathbf{R}}, t)}$, we have, in the limit of negligible NAC, (see Eq. (S.18) in the SM for the general case)

$$\begin{aligned} \partial_t |\Gamma_{jk}(\underline{\mathbf{R}}, t)| &= -|\Gamma_{jk}(\underline{\mathbf{R}}, t)| \sum_{\nu} \left\{ \frac{(\nabla_{\nu} - 2\overline{\mathfrak{S}}_{\nu,jk}) \cdot \mathbf{J}_{\nu}}{|\chi|^2} \right. \\ &\quad \left. + \sum_n \frac{|C_n|^2}{2M_{\nu}} \left[\left(4\mathfrak{Q}_{\nu,jk} - 2\nabla_{\nu} \right) \cdot (\mathbf{f}_{\nu,n} - \mathbf{f}_{\nu,jk}) + 4\mathfrak{S}_{\nu,n} \cdot \mathbf{f}_{\nu,n} \right] \right\} \quad (4) \end{aligned}$$

In Eq. 4, all quantities on the right are functions of $\underline{\mathbf{R}}$ and t , an overline indicates the average over j, k ($\overline{g}_{jk} = (g_j + g_k)/2$), and we have defined $\mathbf{f}_{\nu,k} = \nabla_{\nu}(S_k - S)$. Further, we defined the nuclear quantum momentum \mathbf{Q}_{ν} and projected components $\mathfrak{Q}_{\nu,k}$ for each state k through

$$\mathbf{Q}_{\nu} = -\frac{\nabla_{\nu} |\chi(\underline{\mathbf{R}}, t)|}{|\chi(\underline{\mathbf{R}}, t)|} \quad \text{and} \quad \mathfrak{Q}_{\nu,k}(\underline{\mathbf{R}}, t) = -\frac{\nabla_{\nu} |\chi_k(\underline{\mathbf{R}}, t)|}{|\chi_k(\underline{\mathbf{R}}, t)|} \quad (5)$$

while $\mathfrak{S}_{\nu,k}$ is the “reduced” contribution

$$\mathfrak{S}_{\nu,k}(\underline{\mathbf{R}}, t) = -\frac{\nabla_{\nu} |C_k(\underline{\mathbf{R}}, t)|}{|C_k(\underline{\mathbf{R}}, t)|} = \mathfrak{Q}_{\nu,k} - \mathbf{Q}_{\nu} \quad (6)$$

with $C_k(\underline{\mathbf{R}}, t) = \chi_k(\underline{\mathbf{R}}, t)/\chi(\underline{\mathbf{R}}, t)$, which represent coefficients of the conditional electronic wavefunction $\Phi_{\underline{\mathbf{R}}}(\underline{\mathbf{r}}, t)$ when expanded in the BO basis, $\Phi_{\underline{\mathbf{R}}}(\underline{\mathbf{r}}, t) = \sum_n C_n(\underline{\mathbf{R}}, t) \Phi_{\underline{\mathbf{R}},n}(\underline{\mathbf{r}})$.

Our third key observation follows from Eq. (4): While the first term on the right represents a convective contribution to the time-derivative (see more shortly), *both the projected quantum momentum $\mathfrak{Q}_{\nu,k}$ and the reduced contribution $\mathfrak{S}_{\nu,k}$, play a crucial role in capturing accurate spatially-resolved populations and coherences, when away from NAC regions.* The only other term driving (the magnitude of) the coherence or population evolution, $\sum_n |C_n|^2 \nabla_{\nu} \cdot (\mathbf{f}_{\nu,k} + \mathbf{f}_{\nu,j} - 2\mathbf{f}_{\nu,n}) = \sum_n |C_n|^2 \nabla_{\nu}^2 (S_k + S_j -$

$2S_n$), depends on differences in curvature of the adiabatic phases, which semiclassically relates to the curvatures of the BO surfaces (see more shortly). A fourth key observation is that *in regions where the coherence between two states has locally collapsed to zero, only the terms depending on $\mathfrak{S}_{\nu,j(k)}$ survive to drive time-evolution of the spatially-resolved coherences and populations; thus, this is responsible for recoherence effects away from NACs, and will be discussed in more detail shortly.*

The unique and unambiguous definition of the total nuclear density and current-density rooted in the EF, allows us to derive an *exact trajectory-based* equation from Eq. (4). We represent the nuclear density as a sum over δ -functions (or very narrow Gaussians) centered at a trajectory position $\underline{\mathbf{R}}^{(I)}(t)$

$$|\chi(\underline{\mathbf{R}}, t)|^2 \rightarrow \frac{1}{N_{tr}} \sum_I \delta(\underline{\mathbf{R}} - \underline{\mathbf{R}}^{(I)}(t)) \quad (7)$$

where $\underline{\mathbf{R}}^{(I)}(t)$ satisfy classical Newton's equations [21, 22] with a generalized Lorentz force dependent on $\Phi_{\underline{\mathbf{R}}}$ [26–28]. The gradient of the phase S becomes $\nabla_{\nu} S \rightarrow M_{\nu} \dot{\underline{\mathbf{R}}}(t) - \mathbf{A}$ where \mathbf{A} is the vector potential in the nuclear Hamiltonian (see SM), and the time-derivative along the trajectory given by the convective derivative $d/dt = \partial_t + \sum_{\nu} \dot{\underline{\mathbf{R}}}_{\nu}^{(I)} \cdot \nabla_{\nu}$. The spatially-resolved and -averaged coherences and populations become trajectory-ensembles:

$$\begin{aligned} \Gamma_{jk}(\underline{\mathbf{R}}, t) &\rightarrow \frac{1}{N_{tr}} \sum_I \delta(\underline{\mathbf{R}} - \underline{\mathbf{R}}^{(I)}(t)) C_j^{(I)*}(t) C_k^{(I)}(t) \\ \Gamma_{jk}(t) &\rightarrow \sum_I C_j^{(I)*}(t) C_k^{(I)}(t) \end{aligned} \quad (8)$$

Then Eq. 4 becomes

$$\begin{aligned} \frac{d|C_j^* C_k|^{(I)}}{dt} &= - \left| C_j^{*(I)} C_k^{(I)} \right| \sum_{\nu,n} \frac{|C_n^{(I)}|^2}{2M_{\nu}} \\ &\left[\left(4\mathfrak{Q}_{\nu,jk}^{(I)} - 2\nabla_{\nu} \right) \cdot \left(\mathbf{f}_{\nu,n}^{(I)} - \mathbf{f}_{\nu,jk}^{(I)} \right) + 4\mathfrak{S}_{\nu,n}^{(I)} \cdot \mathbf{f}_{\nu,n}^{(I)} \right] \end{aligned} \quad (9)$$

where all are functions of t alone, and we use the shorthand $g^{(I)} = g(\underline{\mathbf{R}}^{(I)}(t))$.

Away from any NAC, Eq. 9 gives the exact equation for the magnitude of the electronic populations and coherences that trajectory-based methods should be aiming for. The full equation including the NACs, and phases, is given in the SM (Eq. (S.33–S.35)). The I -dependence gives the spatially-resolved character in the trajectory-picture: while the electronic populations ($C_j^{*(I)} C_j^{(I)}(t)$) and coherences ($C_j^{*(I)} C_{k \neq j}^{(I)}(t)$) for each individual trajectory evolve in time in the case of parallel surfaces, their sum over trajectories should remain constant in the limit of a large sampling of the initial distribution, analogous to the discussion below Eq. (3). Time-

dependence of the individual $C_k^{(I)}(t)$ indicates spatial-dependence in the coefficients, crucial for getting the correct populations and coherences, even when only ensemble-averaged quantities are measurable, as discussed earlier and as we will see explicitly shortly.

The traditional trajectory-based methods (Ehrenfest, surface-hopping) give strictly zero time-evolution throughout the ensemble when NACs are negligible because they have no non-local quantum momentum terms, and *ad hoc* decoherence corrections to surface-hopping cause spurious decays. Our examples will demonstrate this has drastic consequences for intermediate and long-term coherence and population dynamics. The prime importance of the projected quantum momenta in Eq. 9 is, on the other hand, partially recognized in the EF-based CTMQC method [21, 22], which approximates these terms. Derived from a well-defined series of approximations on the exact electronic and nuclear equations, the resulting CTMQC equations neglect $\mathfrak{S}_{\nu,k}$, effectively approximating $\mathfrak{Q}_{\nu,k}$ by $\mathbf{Q}_{\nu} \forall k, \nu$. We find (again, for negligible NAC)

$$\begin{aligned} \left(\frac{d|C_j^* C_k|}{dt} \right)_{\text{exact}}^{(I)} &= \left(\frac{d|C_j^* C_k|}{dt} \right)_{\text{CTMQC}}^{(I)} + |C_j^{*(I)} C_k^{(I)}| \\ &\sum_{\nu,n} \frac{|C_n^{(I)}|^2}{2M_{\nu}} \left[\left(4\mathfrak{S}_{\nu,jk}^{(I)} - 2\nabla_{\nu} \right) \cdot \left(\mathbf{f}_{\nu,n}^{(I)} - \mathbf{f}_{\nu,jk}^{(I)} \right) + 4\mathfrak{S}_{\nu,n}^{(I)} \cdot \mathbf{f}_{\nu,n}^{(I)} \right] \end{aligned} \quad (10)$$

This expression assumes the semiclassical approximation for the gradient of the phase of the electronic coefficients $\mathbf{f}_{\nu,l}^{(I)} = -\int_0^t \nabla_{\nu} E_l^{(I)} dt$, valid away from NACs [22].

A consequence of CTMQC's neglect of \mathfrak{S} would be spurious population transfer in regions of zero NAC that is however fixed in implementations by redefining the quantum momentum to enforce no net transfer in these cases [21, 22, 40]. However, another consequence, that is not fixed by this redefinition, is CTMQC's inability to capture recoherence away from NAC regions as noted in the fourth observation made earlier. Consider the situation where, at some time t , $C_k^{(I)}(t) = 0$ for trajectory I and $C_j^{(J)}(t) = 0$ for trajectory J . If the forces on the nuclei cause the two trajectories to move to the same spatial region, the magnitude of the coherence $\Gamma_{jk}(t)$ should increase from zero for both these trajectories. Now, in the exact trajectory equation Eq. (9) for trajectory I , the $|C_k^{(I)}(t)|$ in front of the sum on the right sets all terms to zero except for the term involving $\mathfrak{Q}_{\nu,k}^{(I)}$ since in that term $|C_k^{(I)}(t)|$ is in the denominator:

$$\frac{d}{dt} |C_j^* C_k|^{(I)} = |C_j^{(I)}| \sum_{\nu} \sum_n \frac{2|C_n^{(I)}|^2}{M_{\nu}} \nabla_{\nu} |C_k^{(I)}| \cdot \left(\mathbf{f}_{\nu,n}^{(I)} - \mathbf{f}_{\nu,k}^{(I)} \right) \quad (11)$$

This is non-zero when for a neighboring trajectory J , $C_k^{(J)}(t) \neq 0$, (i.e. $\nabla_\nu |C_k| \neq 0$). This spatial-dependence of the coefficients, contained in the reduced projected quantum momentum $\mathfrak{S}_{k,\nu}$, is key to the growth of the coherence. CTMQC neglects this term and as a result, CTMQC fails to capture recoherence.

Our first example, EL20-SAC, consists of two parallel electronic states that eventually reach a single avoided crossing (SAC) [15], and a third non-parallel state uncoupled to the others [20] (inset of Fig. 1). The Hamiltonian is given in the SM.

The system is initialized in a 50 : 25 : 25 coherent superposition of three gaussian nuclear wavepackets with center momentum 40 bohr⁻¹ and position -26 bohr. The model illustrates fundamental aspects of electronic coherences. First, their pair-wise nature [20]: coherence between the pair of parallel states should be maintained while coherence between non-parallel states should be lost due to diverging wavepackets. Second, the need to accurately describe the spatially-resolved coherence, as this is key to correctly capture the dynamics even of spatially-averaged quantities, when later entering into the NAC region.

Figure 1 shows the magnitude of the spatially-averaged electronic coherences [41] and first-excited population, obtained from Ehrenfest (EHREN), surface-hopping with energy-based decoherence correction (SHEDC) [42, 43], EF-based CTMQC, EF-based surface-hopping (SHXF) [23, 44], and the exact calculations. Consider first before the SAC is reached. As expected, Ehrenfest captures the spatially-averaged coherence between the parallel surfaces but fails to capture the decoherence between the non-parallel surfaces, while in SHEDC the parallel coherence erroneously decays and the non-parallel decays much too quickly. Instead, CTMQC does a good job for both. The more approximate SHXF predicts too long non-parallel coherence decay time, and the parallel coherence shows some deviation from constant. All methods capture the (trajectory-averaged) populations well at early times. However, once they reach the SAC, only CTMQC reasonably captures the population and coherence dynamics at the right time, albeit with an overestimation, before settling to about the right values. SHXF gets the trend in the right direction, but the timing and duration of the event is too long. The traditional trajectory-based methods are completely wrong: SHEDC shows hardly any transfer and wrong coherence behavior, and Ehrenfest's population goes in the wrong direction. We note that the thawed Gaussian approach of Ref. [14], not shown here, would approximate the early behavior well but has no mechanism to include NAC coupling.

Why the spatially-averaged electronic quantities are poor at later times in the traditional trajectory-based methods is revealed by inspecting the spatially-resolved

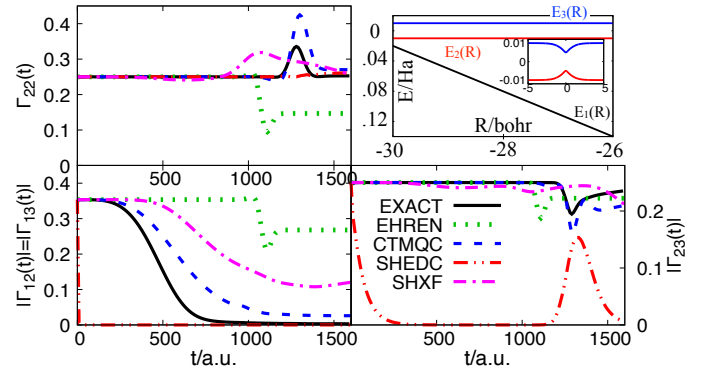


FIG. 1. Electronic state populations of the first excited state (top left), adiabatic PES (top right), magnitude of electronic coherences between non-parallel states 1 and 2 (or 3) (bottom left) and parallel states 2 and 3 (bottom right) for EL20-SAC. The NAC is only non-zero near the SAC localized at $R = 0$.

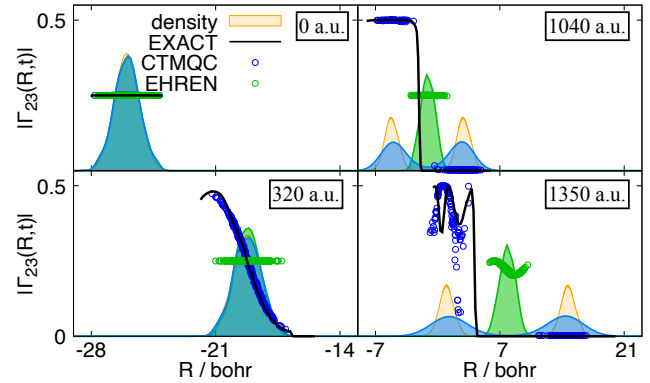


FIG. 2. Snapshots of the exact density (orange shaded), density reconstructed from the distribution of CTMQC (blue shaded) and Ehrenfest trajectories (green shaded) and corresponding spatially-resolved coherences between the two parallel surfaces.

quantities at earlier times, as plotted in Fig. 2. Even before there is a clear splitting between the wavepackets on non-parallel surfaces (e.g. $t = 320$ a.u.), we see a distinct curvature in the exact spatially-resolved coherence (also in populations, not shown), captured well by CTMQC but completely missed in Ehrenfest which remains structureless until the avoided crossing region. The projected quantum-momentum terms in the equation of motion create this spatial structure; these terms are well-approximated by CTMQC but absent in the traditional methods, yet the latter correctly ensemble-average to zero before the SAC is reached. The incorrect spatial structure in Ehrenfest and SHEDC lead to incorrect ensemble-averaged populations and coherences at later times, since trajectories enter the SAC with wrong coefficients.

The second model, denoted 3HO, consists of three uncoupled harmonic oscillators, two of which are par-

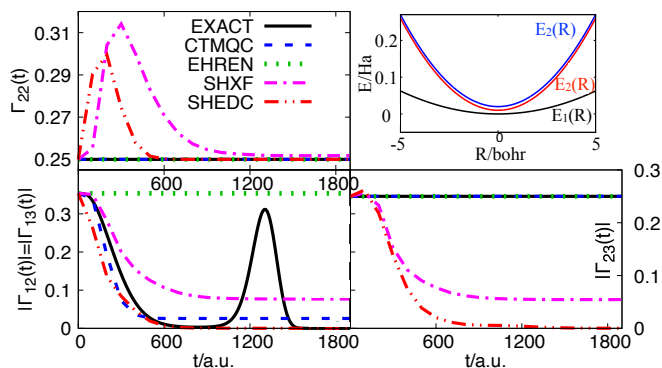


FIG. 3. As in Fig. 1, but for the 3HO model.

allel (inset of Fig. 3); the Hamiltonian is given in the SM. The system is initialized in a 50 : 25 : 25 coherent superposition of three gaussian nuclear wavepackets with zero momentum centered at -4 bohr. While the wavepackets on the parallel surfaces maintain constant coherence, they show successive decoherences and recoherences with the wavepacket on the non-parallel surface. Figure 3 shows that, again, while Ehrenfest maintains coherence between all states, SHEDC shows decoherence for all. SHXF shows similar behavior to SHEDC, and both suffer from spurious population transfer [38]. CTMQC on the other hand, correctly captures the first decoherence event while maintaining constant spatially-averaged coherences between the parallel surfaces, and correctly constant populations, due its redefinition of the quantum momentum preventing spurious net transfer. However, the recoherence is absent in all the methods, and would also be in the thawed Gaussian approach (not shown). This is because we enter the domain of the fourth observation made earlier and Eq. (11), where, after the first decoherence, the \mathfrak{S}_n are the only terms that can drive coherence change, and is missing in all approaches. The importance of \mathfrak{S}_n is evident from the snapshots of the exact Q , Q_1 and \mathfrak{S}_1 shown in the SM (Fig. S.1), where \mathfrak{S} displays large features that largely cancel those in Q , crunching it down to yield a relatively small Q_k .

In summary, we identified the key role played by the projected nuclear quantum momentum, a signature of electron-nuclear correlation missed in earlier analyses, in determining the correct spatially-resolved electronic coherence, and the importance of spatial-resolution in influencing subsequent spatially-averaged coherences. The EF approach allows the definition of exact trajectory-based equations for the electronic coefficients, thanks to the notion of a single nuclear wavefunction with the correct density and current-density. Unlike traditional trajectory-based methods, the EF-based CTMQC is promising for simulating electronic coherences in molecules, because it approximates the pro-

jected nuclear quantum momentum, and accurately predicts coherences and populations in models in which traditional trajectory-based methods fail, distinguishing coherence between parallel surfaces and decoherence between non-parallel. Future work will explore a correction to CTMQC that reinstates the neglected \mathfrak{S}_n , which should then capture recoherence, while simultaneously eliminating the need for redefining the quantum momentum.

We gratefully acknowledge financial aid from the National Science Foundation Award No. CHE- 2154829, and the Department of Energy, Office of Basic Energy Sciences, Division of Chemical Sciences, Geosciences and Biosciences under Award No. DE-SC0020044, the Computational Chemistry Center: Chemistry in Solution and at Interfaces funded by the U.S. Department of Energy, Office of Science Basic Energy Sciences, under Award No. DE-SC0019394.

-
- [1] Brian Kaufman, Philipp Marquetand, Tamás Rozgonyi, and Thomas Weinacht, "Long-lived electronic coherences in molecules," *Phys. Rev. Lett.* **131**, 263202 (2023).
 - [2] M. Garg, A. Martin-Jimenez, M. Pizarra, Y. Luo, F. Martín, and K. Kern, "Real-space subfemtosecond imaging of quantum electronic coherences in molecules," *Nature Photonics* **16**, 196–202 (2022).
 - [3] Gönen MC Mogol, Brian Kaufman, Thomas Weinacht, Chuan Cheng, and Itzik Ben-Itzhak, "Direct observation of entangled electronic-nuclear wave packets," *Phys. Rev. Res.* **6**, L022047 (2024).
 - [4] Victor Despré, Nikolay V. Golubev, and Alexander I. Kuleff, "Charge migration in propionic acid: A full quantum dynamical study," *Phys. Rev. Lett.* **121**, 203002 (2018).
 - [5] Diptesh Dey, Alexander I. Kuleff, and Graham A. Worth, "Quantum interference paves the way for long-lived electronic coherences," *Phys. Rev. Lett.* **129**, 173203 (2022).
 - [6] Morgane Vacher, Michael J. Bearpark, Michael A. Robb, and João Pedro Malhado, "Electron dynamics upon ionization of polyatomic molecules: Coupling to quantum nuclear motion and decoherence," *Phys. Rev. Lett.* **118**, 083001 (2017).
 - [7] HG Duan, VI Prokhorenko, RJ Cogdell, K Ashraf, AL Stevens, M Thorwart, and RJD Miller, "Nature does not rely on long-lived electronic quantum coherence for photosynthetic energy transfer," *Proc. Natl. Acad. Sci.* **114** (2017).
 - [8] Margherita Maiuri, Evgeny E. Ostroumov, Rafael G. Saer, Robert E. Blankenship, and Gregory D. Scholes, "Coherent wavepackets in the fenna–matthews–olson complex are robust to excitonic-structure perturbations caused by mutagenesis," *Nat. Chem.* **10**, 177–183 (2018).
 - [9] Michael R. Wasielewski, Malcolm D. E. Forbes, Natia L. Frank, Karol Kowalski, Gregory D. Scholes, Joel Yuen-Zhou, Marc A. Baldo, Danna E. Freedman, Randall H. Goldsmith, Theodore Goodson, Martin L. Kirk, James K. McCusker, Jennifer P. Ogilvie, David A. Shultz, Stefan Stoll, and K. Birgitta Whaley, "Exploiting chemistry and molecular systems for quantum information science,"

- Nature Reviews Chemistry 4, 490–504 (2020).
- [10] Evaristo Villaseco Arribas, Neepa T. Maitra, and Federica Agostini, “Nonadiabatic dynamics with classical trajectories: The problem of an initial coherent superposition of electronic states,” *J. Chem. Phys.* **160**, 054102 (2024), <https://pubs.aip.org/aip/jcp/article-pdf/doi/10.1063/5.0186984/19333721/054102.1.5.0186984.pdf>.
- [11] Zheng Li, Sandeep Gyawali, Anatoly A. Ischenko, Stuart Hayes, and R. J. Dwayne Miller, “Mapping atomic motions with electrons: Toward the quantum limit to imaging chemistry,” *ACS Photonics* **7**, 296–320 (2020), <https://doi.org/10.1021/acsp Photonics.9b01008>.
- [12] SM Cavaletto, D Keefer, JR Rouxel, F Aleotti, F Segatta, M Garavelli, and S. Mukamel, “Unveiling the spatial distribution of molecular coherences at conical intersections by covariance x-ray diffraction signals,” *Proc. Natl. Acad. Sci.* **118** (2021).
- [13] Gregory A. Fiete and Eric J. Heller, “Semiclassical theory of coherence and decoherence,” *Phys. Rev. A* **68**, 022112 (2003).
- [14] Nikolay V. Golubev, Tomislav Begušić, and Jiří Vaníček, “On-the-fly ab initio semiclassical evaluation of electronic coherences in polyatomic molecules reveals a simple mechanism of decoherence,” *Phys. Rev. Lett.* **125**, 083001 (2020).
- [15] J. C. Tully, “Molecular dynamics with electronic transitions,” *J. Chem. Phys.* **93**, 1061–1071 (1990).
- [16] J. C. Tully, “Mixed quantum-classical dynamics,” *Faraday Discuss.* **110**, 407–419 (1998).
- [17] Linjun Wang, Alexey Akimov, and Oleg V. Prezhdo, “Recent Progress in Surface Hopping: 2011–2015,” *J. Phys. Chem. Lett.* **7**, 2100–2112 (2016).
- [18] Rachel Crespo-Otero and Mario Barbatti, “Recent Advances and Perspectives on Nonadiabatic Mixed Quantum–Classical Dynamics,” *Chem. Rev.* **118**, 7026–7068 (2018).
- [19] Joseph E. Subotnik, Amber Jain, Brian Landry, Andrew Petit, Wenjun Ouyang, and Nicole Bellonzi, “Understanding the Surface Hopping View of Electronic Transitions and Decoherence,” *Ann. Rev. Phys. Chem.* **67**, 387–417 (2016).
- [20] Michael P. Esch and Benjamin G. Levine, “State-pairwise decoherence times for nonadiabatic dynamics on more than two electronic states,” *J. Chem. Phys.* **152**, 234105 (2020).
- [21] Seung Kyu Min, Federica Agostini, and E. K. U. Gross, “Coupled-Trajectory Quantum-Classical Approach to Electronic Decoherence in Nonadiabatic Processes,” *Phys. Rev. Lett.* **115**, 073001 (2015).
- [22] Federica Agostini, Seung Kyu Min, Ali Abedi, and E. K. U. Gross, “Quantum-Classical Nonadiabatic Dynamics: Coupled- vs Independent-Trajectory Methods,” *J. Chem. Theory Comput.* **12**, 2127–2143 (2016).
- [23] Jong-Kwon Ha, In Seong Lee, and Seung Kyu Min, “Surface Hopping Dynamics beyond Nonadiabatic Couplings for Quantum Coherence,” *J. Phys. Chem. Lett.* **9**, 1097–1104 (2018).
- [24] Evaristo Villaseco Arribas and Neepa T. Maitra, “Energy-conserving coupled trajectory mixed quantum-classical dynamics,” *J. Chem. Phys.* **158**, 161105 (2023).
- [25] Lucien Dupuy, Anton Rikus, and Neepa T. Maitra, “Exact-factorization-based surface hopping without velocity adjustment,” *The Journal of Physical Chemistry Letters* **15**, 2643–2649 (2024).
- [26] Chen Li, Ryan Requist, and E. K. U. Gross, “Energy, momentum, and angular momentum transfer between electrons and nuclei,” *Phys. Rev. Lett.* **128**, 113001 (2022).
- [27] F. Agostini, A. Abedi, and E. K. U. Gross, “Classical nuclear motion coupled to electronic non-adiabatic transitions,” *J. Chem. Phys.* **141**, 214101 (2014).
- [28] A. Abedi, F. Agostini, and E. K. U. Gross, “Mixed quantum-classical dynamics from the exact decomposition of electron-nuclear motion,” *Europhys. Lett.* **106**, 33001 (2014).
- [29] Geoffrey Hunter, “Conditional probability amplitudes in wave mechanics,” *Int. J. Quantum Chem.* **9**, 237 (1975).
- [30] Geoffrey Hunter, “Ionization potentials and conditional amplitudes,” *Int. J. Quantum Chem.* **9**, 311 (1975).
- [31] Geoffrey Hunter, “Nodeless wave function quantum theory,” *Int. J. Quantum Chem.* **9**, 133 (1980).
- [32] Geoffrey Hunter, “Nodeless wave functions and spiky potentials,” *Int. J. Quantum Chem.* **19**, 755 (1981).
- [33] Geoffrey Hunter and Chin Chui Tai, “Variational marginal amplitudes,” *Int. J. Quantum Chem.* **21**, 1041 (1982).
- [34] Nikitas I. Gidopoulos and E. K. U. Gross, “Electronic non-adiabatic states: towards a density functional theory beyond the Born–Oppenheimer approximation,” *Philosophical Transactions of the Royal Society of London A: Mathematical, Physical and Engineering Sciences* **372** (2014).
- [35] Ali Abedi, Neepa T. Maitra, and E. K. U. Gross, “Exact Factorization of the Time-Dependent Electron-Nuclear Wave Function,” *Phys. Rev. Lett.* **105**, 123002 (2010).
- [36] Ali Abedi, Neepa T. Maitra, and E. K. U. Gross, “Correlated electron-nuclear dynamics: Exact factorization of the molecular wavefunction,” *J. Chem. Phys.* **137**, 22A530 (2012).
- [37] Federica Agostini and E. K. U. Gross, “Ultrafast dynamics with the exact factorization,” *Eur. Phys. J. B* **94**, 179 (2021).
- [38] Evaristo Villaseco Arribas, Federica Agostini, and Neepa T. Maitra, “Exact Factorization Adventures: A Promising Approach for Non-Bound States,” *Molecules* **27**, 13 (2022).
- [39] See Supplemental Material which includes Refs. [10, 21, 26–38, 44–52].
- [40] Seung Kyu Min, Federica Agostini, Ivano Tavernelli, and E. K. U. Gross, “Ab Initio Nonadiabatic Dynamics with Coupled Trajectories: A Rigorous Approach to Quantum (De)Coherence,” *J. Phys. Chem. Lett.* **8**, 3048–3055 (2017).
- [41] Note that here we have shown $\int |\Gamma_{ij}(R, t)| dR$ as the magnitude of the coherence, rather than $|\int \Gamma_{ij}(R, t) dR|$, i.e. the measure we are showing does not include dephasing.
- [42] G. Granucci and M. Persico, “Critical appraisal of the fewest switches algorithm for surface hopping,” *J. Chem. Phys.* **126**, 134114 (2007).
- [43] Giovanni Granucci, Maurizio Persico, and Alberto Zocante, “Including quantum decoherence in surface hopping,” *J. Chem. Phys.* **133**, 134111 (2010).
- [44] In Seong Lee, Jong-Kwon Ha, Daeho Han, Tae In Kim, Sung Wook Moon, and Seung Kyu Min, “PyUNIXMD: A Python-based excited state molecular dynamics package,” *J. Comput. Chem.* **42**, 1755–1766 (2021).
- [45] F. Agostini, I. Tavernelli, and G. Ciccotti, “Nuclear Quantum Effects in Electronic (Non)Adiabatic Dynamics,” *Euro. Phys. J. B* **91**, 139 (2018).
- [46] G. A. Worth, M. A. Robb, and I. Burghardt, “A novel algorithm for non-adiabatic direct dynamics using varia-

- tional gaussian wavepackets," *Faraday Discuss.* **127**, 307–323 (2004).
- [47] M. Ben-Nun and Todd J. Martinez, "Nonadiabatic molecular dynamics: Validation of the multiple spawning method for a multidimensional problem," *J. Chem. Phys.* **108**, 7244–7257 (1998).
- [48] M. Ben-Nun, Jason Quenneville, and Todd J. Martínez, "Ab Initio Multiple Spawning: Photochemistry from First Principles Quantum Molecular Dynamics," *J. Phys. Chem. A* **104**, 5161–5175 (2000).
- [49] Dmitrii V. Shalashilin, "Quantum mechanics with the basis set guided by ehrenfest trajectories: Theory and application to spin-boson model," *J. Chem. Phys.* **130**, 244101 (2009).
- [50] Dmitry V. Makhov, Christopher Symonds, Sebastian Fernandez-Alberti, and Dmitrii V. Shalashilin, "Ab initio quantum direct dynamics simulations of ultrafast photochemistry with multiconfigurational ehrenfest approach," *Chemical Physics* **493**, 200–218 (2017).
- [51] Dmitry V. Makhov, William J. Glover, Todd J. Martinez, and Dmitrii V. Shalashilin, "Ab initio multiple cloning algorithm for quantum nonadiabatic molecular dynamics," *J. Chem. Phys.* **141**, 054110 (2014).
- [52] Federica Agostini, Emmanuele Marsili, Francesco Talotta, Evaristo Villaseco Arribas, Lea Maria Ibele, and Eduarda. Sangiogo Gil, "G-CTMQC," (Last accessed Oct 2023).

SUPPLEMENTARY MATERIAL

SM.1 EXACT FACTORIZATION OF THE MOLECULAR WAVEFUNCTION

The full time-dependent molecular wavefunction can be exactly factorized as a single correlated product [29–38], $\Psi(\underline{\mathbf{r}}, \underline{\mathbf{R}}, t) = \chi(\underline{\mathbf{R}}, t)\Phi_{\underline{\mathbf{R}}}(\underline{\mathbf{r}}, t)$ where the electronic wavefunction satisfies the partial normalization condition $\int |\Phi_{\underline{\mathbf{R}}}(\underline{\mathbf{r}}, t)|^2 d\underline{\mathbf{r}} = 1 \forall \underline{\mathbf{R}}, t$. The marginal factor $\chi(\underline{\mathbf{R}}, t) = e^{iS(\underline{\mathbf{R}}, t)}|\chi(\underline{\mathbf{R}}, t)|$ is interpreted as a nuclear wavefunction because its modulus-square gives the exact nuclear density and the gradient of its phase the exact nuclear current-density (and nuclear velocity field) of the molecular wavefunction:

$$|\chi(\underline{\mathbf{R}}, t)|^2 = \int |\Psi(\underline{\mathbf{r}}, \underline{\mathbf{R}}, t)|^2 d\underline{\mathbf{r}} \quad (\text{S.12})$$

$$\mathbf{V}(\underline{\mathbf{R}}, t) = \frac{\nabla_{\nu} S(\underline{\mathbf{R}}, t)}{M_{\nu}} = \frac{\mathbf{J}_{\nu}(\underline{\mathbf{R}}, t)}{|\chi(\underline{\mathbf{R}}, t)|^2} - \frac{\mathbf{A}_{\nu}(\underline{\mathbf{R}}, t)}{M_{\nu}} \quad (\text{S.13})$$

with $M_{\nu}\mathbf{J}_{\nu}(\underline{\mathbf{R}}, t) = \text{Im}\langle\Psi(\underline{\mathbf{R}}, t)|\nabla_{\nu}\Psi(\underline{\mathbf{R}}, t)\rangle_{\underline{\mathbf{r}}}$. The time-evolution for the electronic and nuclear subsystems satisfy

$$i\partial_t\chi(\underline{\mathbf{R}}, t) = \hat{H}_N(\underline{\mathbf{R}}, t)\chi(\underline{\mathbf{R}}, t) \quad (\text{S.14})$$

$$i\partial_t\Phi_{\underline{\mathbf{R}}}(\underline{\mathbf{r}}, t) = \left[\hat{H}_{el}(\underline{\mathbf{r}}, \underline{\mathbf{R}}) - \epsilon(\underline{\mathbf{R}}, t)\right]\Phi_{\underline{\mathbf{R}}}(\underline{\mathbf{r}}, t) \quad (\text{S.15})$$

The nuclear equation is of Schrödinger form with Hamiltonian

$$\hat{H}_N(\underline{\mathbf{R}}, t) = \sum_{\nu} \frac{(-i\nabla_{\nu} + \mathbf{A}_{\nu}(\underline{\mathbf{R}}, t))^2}{M_{\nu}} + \epsilon(\underline{\mathbf{R}}, t). \quad (\text{S.16})$$

The scalar $\epsilon(\underline{\mathbf{R}}, t) = \langle\Phi_{\underline{\mathbf{R}}}(t)|\hat{H}_{el} - i\partial_t|\Phi_{\underline{\mathbf{R}}}(t)\rangle_{\underline{\mathbf{r}}}$ and vector potentials $\mathbf{A}_{\nu}(\underline{\mathbf{R}}, t) = -i\langle\Phi_{\underline{\mathbf{R}}}(t)|\nabla_{\nu}\Phi_{\underline{\mathbf{R}}}(t)\rangle_{\underline{\mathbf{r}}}$ incorporate the effect of the electronic wavefunction in the nuclear subsystem. On the other hand, the electronic equation is non-linear with electronic Hamiltonian defined as

$$\hat{H}_{el}(\underline{\mathbf{r}}, \underline{\mathbf{R}}) = \hat{H}_{BO}(\underline{\mathbf{r}}; \underline{\mathbf{R}}) + \hat{U}_{eN}[\Phi_{\underline{\mathbf{R}}}, \chi] \quad (\text{S.17})$$

and electron-nuclear coupling operator defined as

$$\hat{U}_{eN} = \sum_{\nu} \frac{1}{M_{\nu}} \left[\frac{(-i\nabla_{\nu} - \mathbf{A}_{\nu}(\underline{\mathbf{R}}, t))^2}{2} + \left(\frac{-i\nabla_{\nu}\chi(\underline{\mathbf{R}}, t)}{\chi(\underline{\mathbf{R}}, t)} + \mathbf{A}_{\nu}(\underline{\mathbf{R}}, t) \right) (-i\nabla_{\nu} - \mathbf{A}_{\nu}(\underline{\mathbf{R}}, t)) \right] \quad (\text{S.18})$$

which incorporates the effect of the nuclear wavefunction in the electronic subsystem.

Note that the factorized form of $\Psi(\underline{\mathbf{r}}, \underline{\mathbf{R}}, t)$ is exact and unique up to a $\underline{\mathbf{R}}$ and t dependent phase, i.e $\tilde{\chi}(\underline{\mathbf{R}}, t) \rightarrow e^{i\theta(\underline{\mathbf{R}}, t)}\chi(\underline{\mathbf{R}}, t)$, $\tilde{\Phi}_{\underline{\mathbf{R}}}(\underline{\mathbf{r}}, t) \rightarrow e^{-i\theta(\underline{\mathbf{R}}, t)}\Phi_{\underline{\mathbf{R}}}(\underline{\mathbf{r}}, t)$, $\tilde{\Psi}(\underline{\mathbf{r}}, \underline{\mathbf{R}}, t) \rightarrow \Psi(\underline{\mathbf{r}}, \underline{\mathbf{R}}, t)$, with $\epsilon(\underline{\mathbf{R}}, t)$ and $\mathbf{A}_{\nu}(\underline{\mathbf{R}}, t)$ transforming according to standard electrodynamic potentials $\tilde{\mathbf{A}}_{\nu}(\underline{\mathbf{R}}, t) \rightarrow \mathbf{A}_{\nu}(\underline{\mathbf{R}}, t) + \nabla_{\nu}\theta(\underline{\mathbf{R}}, t)$ and $\tilde{\epsilon}(\underline{\mathbf{R}}, t) = \epsilon(\underline{\mathbf{R}}, t) + \partial_t\theta(\underline{\mathbf{R}}, t)$.

Although the single-product form of the exact factorization (EF) approach resembles the form of the molecular wavefunction in the Born-Oppenheimer approximation, a significant distinction is that in the former, the equations for the electronic and nuclear wavefunctions must be solved self-consistently, while in the latter, the electronic equation can be solved first for each $\underline{\mathbf{R}}$ and then the nuclear equation solved.

While both the Born-Huang expansion and the exact factorization approach are formally exact, the advantage of using the exact factorization approach for these problems is that it enables the definition of a unique unambiguous force [21, 26–28, 45] that drives nuclear trajectories in mixed quantum-classical (MQC) schemes. This force incorporates coupling to electrons (and any external fields) in a rigorous way. While the Born-Huang expansion also gives a formally exact representation of the molecular wavefunction, it is more challenging to derive a consistent set of equations in MQC schemes because nuclear wavepackets on different electronic surfaces experience different forces, which gives ambiguity to the force on a classical trajectory at a given nuclear position. For example, Ehrenfest simply takes an average of the adiabatic forces, weighted by the electronic coefficients, but this mean-field force cannot yield wavepacket splitting, becoming increasingly unphysical away from regions of strong electron-nuclear coupling (avoided or conical intersections). To avoid this, the surface hopping scheme instead uses an adiabatic

force at all times, but to account for coupling must stochastically hop between active states. While there are more sophisticated trajectory-based schemes stemming from the Born-Huang expansion (e.g. variational multiconfiguration Gaussian [46], ab initio multiple spawning [47, 48], multi-configurational Ehrenfest [49, 50], ab initio multiple cloning [51]), the simplicity and physicality of a single unique nuclear force defined over the ensemble of classical trajectories, with each trajectory associated with quantum electronic coefficients, gives EF-based MQC a particular advantage, conceptually as well as numerically.

SM.2 EXACT EQUATIONS FOR THE EVOLUTION OF ELECTRONIC COHERENCES

The electronic coherence defined in Eq. (1) of the main text, is based on the projected nuclear wavefunctions $\chi_j(\underline{\mathbf{R}}, t)$ in the Born-Huang basis, $\Psi(\underline{\mathbf{r}}, \underline{\mathbf{R}}, t) \stackrel{\text{BO}}{=} \sum_j \chi_j(\underline{\mathbf{R}}, t) \Phi_{\underline{\mathbf{R}}, j}(\underline{\mathbf{r}})$. The full, exact, equation for the time evolution of the magnitude of the electronic coherences of Eq.(1), including non-adiabatic couplings, reads:

$$\begin{aligned} i\partial_t \Gamma_{jk}(\underline{\mathbf{R}}, t) &= \Delta E_{kj}(\underline{\mathbf{R}}) \Gamma_{jk}(\underline{\mathbf{R}}, t) + \sum_{\nu} \frac{1}{2M_{\nu}} \left(\chi_k(\underline{\mathbf{R}}, t) \nabla_{\nu}^2 \chi_j^*(\underline{\mathbf{R}}, t) - \chi_j^*(\underline{\mathbf{R}}, t) \nabla_{\nu}^2 \chi_k(\underline{\mathbf{R}}, t) \right. \\ &\quad - \sum_{n \neq k} [D_{kn, \nu}(\underline{\mathbf{R}}) \Gamma_{jn}(\underline{\mathbf{R}}, t) + 2\chi_j^*(\underline{\mathbf{R}}, t) \mathbf{d}_{kn, \nu}(\underline{\mathbf{R}}) \cdot \nabla_{\nu} \chi_n(\underline{\mathbf{R}}, t)] \\ &\quad \left. + \sum_{n \neq j} [D_{nj, \nu}(\underline{\mathbf{R}}) \Gamma_{nk}(\underline{\mathbf{R}}, t) + 2\chi_k \mathbf{d}_{jn, \nu}(\underline{\mathbf{R}}) \cdot \nabla_{\nu} \chi_n^*(\underline{\mathbf{R}}, t)] \right) \end{aligned} \quad (\text{S.19})$$

where we have assumed real BO states, no geometric phase effects, $\Delta E_{kj} = E_k - E_j$, and where $\mathbf{d}_{nk, \nu}(\underline{\mathbf{R}})$ and $D_{nk, \nu}(\underline{\mathbf{R}})$ are the non-adiabatic coupling vectors $\langle \phi_{\underline{\mathbf{R}}, n} | \nabla_{\nu} \phi_{\underline{\mathbf{R}}, k} \rangle_{\underline{\mathbf{r}}}$ and scalar couplings $\langle \phi_{\underline{\mathbf{R}}, n} | \nabla_{\nu}^2 \phi_{\underline{\mathbf{R}}, k} \rangle_{\underline{\mathbf{r}}}$ respectively. Writing the wavepackets in polar form, i.e $\chi_n(\underline{\mathbf{R}}, t) = |\chi_n(\underline{\mathbf{R}}, t)| e^{iS_n(\underline{\mathbf{R}}, t)}$, we have

$$\nabla_{\nu} \chi_k(\underline{\mathbf{R}}, t) = (i\nabla_{\nu} S_k(\underline{\mathbf{R}}, t) - \mathcal{Q}_{\nu, k}(\underline{\mathbf{R}}, t)) \chi_k(\underline{\mathbf{R}}, t) \quad (\text{S.20})$$

$$\nabla_{\nu}^2 \chi_k(\underline{\mathbf{R}}, t) = (\mathcal{Q}_{\nu, k}(\underline{\mathbf{R}}, t) - 2i\mathcal{Q}_{\nu, k}(\underline{\mathbf{R}}, t) \cdot \nabla_{\nu} S_k(\underline{\mathbf{R}}, t) + i\nabla_{\nu}^2 S_k(\underline{\mathbf{R}}, t) - (\nabla_{\nu} S_k(\underline{\mathbf{R}}, t))^2) \chi_k(\underline{\mathbf{R}}, t) \quad (\text{S.21})$$

where the k-th state projected quantum momentum and quantum potential read

$$\mathcal{Q}_{\nu, k}(\underline{\mathbf{R}}, t) = -\frac{\nabla_{\nu} |\chi_k(\underline{\mathbf{R}}, t)|}{|\chi_k(\underline{\mathbf{R}}, t)|} \quad \text{and} \quad \mathcal{Q}_{\nu, k}(\underline{\mathbf{R}}, t) = \frac{\nabla_{\nu}^2 |\chi_k(\underline{\mathbf{R}}, t)|}{|\chi_k(\underline{\mathbf{R}}, t)|}. \quad (\text{S.22})$$

We now write these quantities in terms of the exact factorization concepts, where we note that

$$\Psi(\underline{\mathbf{r}}, \underline{\mathbf{R}}, t) \stackrel{\text{BO}}{=} \sum_k \chi_k(\underline{\mathbf{R}}, t) \Phi_{\underline{\mathbf{R}}, k}(\underline{\mathbf{r}}) \stackrel{\text{EF}}{=} \chi(\underline{\mathbf{R}}, t) \Phi_{\underline{\mathbf{R}}}^{\text{BO}}(\underline{\mathbf{r}}, t) = \chi(\underline{\mathbf{R}}, t) \sum_k C_k(\underline{\mathbf{R}}, t) \Phi_{\underline{\mathbf{R}}, k}^{\text{BO}}(\underline{\mathbf{r}}) \quad (\text{S.23})$$

where in the last equality the time-dependent conditional electronic wavefunction is represented by its coefficients $\{C_k\}$ in the expansion, which also represent the projected nuclear wavefunction via:

$$\Phi_{\underline{\mathbf{R}}}(\underline{\mathbf{r}}, t) = \sum_k C_k(\underline{\mathbf{R}}, t) \Phi_{\underline{\mathbf{R}}, k}^{\text{BO}}(\underline{\mathbf{r}}) \quad \text{and} \quad \chi_k(\underline{\mathbf{R}}, t) = \chi(\underline{\mathbf{R}}, t) C_k(\underline{\mathbf{R}}, t). \quad (\text{S.24})$$

Writing the nuclear wavefunction χ and the coefficients C_k also in polar form, $\chi(\underline{\mathbf{R}}, t) = |\chi(\underline{\mathbf{R}}, t)| e^{iS(\underline{\mathbf{R}}, t)}$ and $C_k(\underline{\mathbf{R}}, t) = |C_k(\underline{\mathbf{R}}, t)| e^{i\gamma_k}$, Eq. S.24 means we can relate

$$S_k(\underline{\mathbf{R}}, t) = S(\underline{\mathbf{R}}, t) + \gamma_k(\underline{\mathbf{R}}, t) \quad \text{and} \quad |\chi_k(\underline{\mathbf{R}}, t)| = |\chi(\underline{\mathbf{R}}, t)| |C_k(\underline{\mathbf{R}}, t)| \quad (\text{S.25})$$

We define the k-th state reduced quantum momentum as

$$\mathfrak{S}_{\nu, k}(\underline{\mathbf{R}}, t) = -\frac{\nabla_{\nu} |C_k(\underline{\mathbf{R}}, t)|}{|C_k(\underline{\mathbf{R}}, t)|} \quad (\text{S.26})$$

which allows us to write, equivalently to Eq S.20,

$$\nabla_{\nu} C_k(\underline{\mathbf{R}}, t) = (i\nabla_{\nu} \gamma_k(\underline{\mathbf{R}}, t) - \mathfrak{S}_{\nu, k}(\underline{\mathbf{R}}, t)) C_k(\underline{\mathbf{R}}, t) \quad (\text{S.27})$$

Note that the reduced and projected quantum momenta, $\mathfrak{S}_{\nu,k}(\underline{\mathbf{R}}, t)$ and $\mathfrak{Q}_{\nu,k}(\underline{\mathbf{R}}, t)$, are related through the nuclear quantum momentum $\mathbf{Q}_{\nu}(\underline{\mathbf{R}}, t)$

$$\mathbf{Q}_{\nu}(\underline{\mathbf{R}}, t) = -\frac{\nabla_{\nu}|\chi(\underline{\mathbf{R}}, t)|}{|\chi(\underline{\mathbf{R}}, t)|} = \mathfrak{S}_{\nu,k}(\underline{\mathbf{R}}, t) + \mathfrak{Q}_{\nu,k}(\underline{\mathbf{R}}, t) \quad \forall \nu, k \quad (\text{S.28})$$

In terms of these quantities, we write, omitting the dependencies to avoid notational clutter,

$$\begin{aligned} i\partial_t\Gamma_{jk}(\underline{\mathbf{R}}, t) &= \Delta E_{kj}\Gamma_{jk} + \sum_{\nu} \frac{\Gamma_{jk}}{2M_{\nu}} \left(\Delta\mathfrak{Q}_{\nu,jk} + 2i\mathfrak{Q}_{\nu,j}\nabla_{\nu}S_j - i\nabla_{\nu}^2S_j - (\nabla_{\nu}S_j)^2 + 2i\mathfrak{Q}_{\nu,k}\nabla_{\nu}S_k - i\nabla_{\nu}^2S_k + (\nabla_{\nu}S_k)^2 \right) \\ &- \sum_{\nu, n \neq k} \frac{\Gamma_{jn}}{2M_{\nu}} [D_{kn,\nu} + 2i\mathbf{d}_{kn,\nu} \cdot \nabla_{\nu}S_n - 2\mathbf{d}_{kn,\nu} \cdot \mathfrak{Q}_{\nu,n}] + \sum_{\nu, n \neq j} \frac{\Gamma_{nk}}{2M_{\nu}} [D_{nj,\nu} - 2i\mathbf{d}_{jn,\nu} \cdot \nabla_{\nu}S_n - 2\mathbf{d}_{jn,\nu} \cdot \mathfrak{Q}_{\nu,n}] \end{aligned} \quad (\text{S.29})$$

where we define $\Delta g_{jk} = g_j - g_k$ for any quantity. The advantage of writing in terms of exact factorization quantities means we can relate terms to the nuclear density and current-density (with an eventual view towards establishing a mixed quantum-classical method): from Eq. S.13, the inline equation for \mathbf{A}_{ν} below Eq. (S.5), and the expansion in Eq. S.24, we have

$$\nabla_{\nu}S = M_{\nu}\mathbf{V}_{\nu} = \frac{M_{\nu}\mathbf{J}_{\nu}}{|\chi|^2} - \mathbf{A}_{\nu} = \frac{M_{\nu}\mathbf{J}_{\nu}}{|\chi|^2} - \sum_l |C_l|^2 \nabla_{\nu}\gamma_l - \text{Im} \sum_{kl} C_l^* C_k \mathbf{d}_{\nu,lk} \quad (\text{S.30})$$

and

$$\begin{aligned} \nabla_{\nu}^2S &= M_{\nu}\mathbf{J}_{\nu} \cdot \nabla_{\nu} \frac{1}{|\chi|^2} + \frac{M_{\nu}\nabla_{\nu} \cdot \mathbf{J}_{\nu}}{|\chi|^2} - \nabla_{\nu} \cdot \mathbf{A}_{\nu} \\ &= \frac{M_{\nu}}{|\chi|^2} (\nabla_{\nu} \cdot \mathbf{J}_{\nu} + 2(\mathfrak{Q}_{\nu,k} - \mathfrak{S}_{\nu,k}) \cdot \mathbf{J}_{\nu}) - \sum_l |C_l|^2 (\nabla_{\nu}^2\gamma_l - 2\mathfrak{S}_{\nu,l}\nabla_{\nu}\gamma_l) - \text{Im} \nabla_{\nu} \cdot \sum_{kl} C_l^* C_k \mathbf{d}_{\nu,lk} \end{aligned} \quad (\text{S.31})$$

where we wrote $\mathbf{Q}_{\nu} = \mathfrak{Q}_{\nu,k} - \mathfrak{S}_{\nu,k}$ (Eq. (S.28)). In regions where the NACs are zero, this gives

$$\begin{aligned} \partial_t\Gamma_{jk}(\underline{\mathbf{R}}, t) &= -i\Delta E_{kj}(\underline{\mathbf{R}})\Gamma_{jk}(\underline{\mathbf{R}}, t) + \sum_{\nu} \frac{\Gamma_{jk}}{2M_{\nu}} \left[-i\Delta\mathfrak{Q}_{\nu,jk} + 2(\mathfrak{Q}_{\nu,j} + \mathfrak{Q}_{\nu,k}) \cdot \left(\frac{M_{\nu}\mathbf{J}_{\nu}}{|\chi(\underline{\mathbf{R}}, t)|^2} - \sum_l |C_l|^2 \nabla_{\nu}\gamma_l \right) \right. \\ &+ 2(\mathfrak{Q}_{\nu,j} \cdot \nabla_{\nu}\gamma_j + \mathfrak{Q}_{\nu,k} \cdot \nabla_{\nu}\gamma_k) - \frac{2M_{\nu}}{|\chi(\underline{\mathbf{R}}, t)|^2} (\nabla_{\nu} \cdot \mathbf{J}_{\nu} + (\mathfrak{Q}_{\nu,k} + \mathfrak{Q}_{\nu,j} - \mathfrak{S}_{\nu,k} - \mathfrak{S}_{\nu,j}) \cdot \mathbf{J}_{\nu}) \\ &+ 2\sum_l |C_l|^2 (\nabla_{\nu}^2\gamma_l - 2\mathfrak{S}_{\nu,l}\nabla_{\nu}\gamma_l) - \nabla_{\nu}^2(\gamma_k + \gamma_j) - i(\nabla_{\nu}\gamma_k)^2 + i(\nabla_{\nu}\gamma_j)^2 \\ &\left. - 2i\Delta\nabla_{\nu}\gamma_{kj} \cdot \left(\frac{M_{\nu}\mathbf{J}_{\nu}}{|\chi(\underline{\mathbf{R}}, t)|^2} - \sum_l |C_l|^2 \nabla_{\nu}\gamma_l \right) \right] \end{aligned} \quad (\text{S.32})$$

Rearranging and defining $\nabla_{\nu}\gamma_k = \mathbf{f}_{\nu,k}$ we obtain

$$\begin{aligned} \partial_t\Gamma_{jk}(\underline{\mathbf{R}}, t) &= -\Gamma_{jk}(\underline{\mathbf{R}}, t) \left\{ i\Delta E_{kj}(\underline{\mathbf{R}}) + \sum_{\nu} \frac{1}{|\chi|^2} \left[\left(i\Delta\mathbf{f}_{kj} \cdot \mathbf{J}_{\nu} + \nabla_{\nu} \cdot \mathbf{J}_{\nu} - (\mathfrak{S}_{\nu,k} + \mathfrak{S}_{\nu,j}) \cdot \mathbf{J}_{\nu} \right) \right. \right. \\ &+ \sum_{\nu} \frac{1}{2M_{\nu}} \left[i\Delta\mathfrak{Q}_{\nu,jk} + \sum_l |C_l|^2 (2\mathfrak{Q}_{\nu,j} - \nabla_{\nu}) \cdot \Delta\mathbf{f}_{\nu,lj} + \sum_l |C_l|^2 (2\mathfrak{Q}_{\nu,k} - \nabla_{\nu}) \cdot \Delta\mathbf{f}_{\nu,lk} \right. \\ &\left. \left. + 4\sum_l |C_l|^2 \mathfrak{S}_{\nu,l} \cdot \mathbf{f}_{\nu,l} + i\mathbf{f}_{\nu,k}^2 - i\mathbf{f}_{\nu,j}^2 - 2i\Delta\mathbf{f}_{\nu,kj} \cdot \sum_l |C_l|^2 \mathbf{f}_{\nu,l} \right] \right\} \end{aligned} \quad (\text{S.33})$$

(where again $\Delta\mathbf{f}_{\nu,lk} = \mathbf{f}_{\nu,l} - \mathbf{f}_{\nu,k}$). We define $\tilde{\Gamma}_{jk} = \Gamma_{jk} e^{i \int^t \alpha_{jk}(\mathbf{r}, t') dt'}$ where

$$\alpha_{jk}(\underline{\mathbf{R}}, t) = \Delta E_{kj} + \sum_{\nu} \frac{\Delta\mathbf{f}_{kj} \cdot \mathbf{J}_{\nu}}{|\chi|^2} + \sum_{\nu} \frac{1}{2M_{\nu}} \left[\Delta\mathfrak{Q}_{\nu,jk} + \Delta(\mathbf{f}_{\nu,kj}^2) - 2\Delta\mathbf{f}_{\nu,kj} \cdot \sum_l |C_l|^2 \mathbf{f}_{\nu,l} \right] \quad (\text{S.34})$$

such that

$$\partial_t \tilde{\Gamma}_{jk}(\underline{\mathbf{R}}, t) = -\tilde{\Gamma}_{jk} \left\{ \sum_{\nu} \frac{(\nabla_{\nu} - 2\overline{\mathfrak{S}}_{\nu,jk}) \cdot \mathbf{J}_{\nu}}{|\chi|^2} + \sum_{\nu,l} \frac{|C_l|^2}{2M_{\nu}} \left[\overline{(4\mathfrak{Q}_{\nu,jk} - 2\nabla_{\nu}) \cdot (\mathbf{f}_{\nu,l} - \mathbf{f}_{\nu,jk})} + 4\mathfrak{S}_{\nu,l} \cdot \mathbf{f}_{\nu,l} \right] \right\} \quad (\text{S.35})$$

where we use the notation $\overline{g_{jk}} = (g_j + g_k)/2$ to indicate an average over electronic states j and k .

We observe that $\frac{d|\tilde{\Gamma}_{jk}|^2}{dt} = 2|\tilde{\Gamma}_{jk}| \frac{d|\tilde{\Gamma}_{jk}|}{dt} = 2\text{Re} \left(\tilde{\Gamma}_{jk}^* \frac{d\tilde{\Gamma}_{jk}}{dt} \right) = -2|\tilde{\Gamma}_{jk}|^2 \{..\}$ where $\{..\}$ indicates the term in the curly brackets of Eq. (S.35), which is real. Then using the fact that the magnitudes of Γ and $\tilde{\Gamma}$ are the same, $\frac{d|\Gamma_{jk}|}{dt} = \frac{d|\tilde{\Gamma}_{jk}|}{dt}$, we find $\frac{d|\Gamma_{jk}|}{dt} = -|\tilde{\Gamma}_{jk}| \{..\} = -|\Gamma_{jk}| \{..\}$, as written in Eq. (4) of the main text. We stress that this is the exact equation for the magnitude of the coherence in the limit of negligible non-adiabatic couplings.

As in the main text, the trajectory-based equation for the populations and coherences follows from these equations by replacing the nuclear density by a sum over delta-functions centered at each member I of the trajectory ensemble

$$|\chi(\underline{\mathbf{R}}, t)|^2 \rightarrow \sum_I^{N_{tr}} (|\chi|^2)^{(I)} = \frac{1}{N_{tr}} \sum_I^{N_{tr}} \delta(\underline{\mathbf{R}} - \underline{\mathbf{R}}^{(I)}(t)) \quad \text{and} \quad (\text{S.36})$$

$$\Gamma_{jk}(\underline{\mathbf{R}}, t) = |\chi(\underline{\mathbf{R}}, t)|^2 C_j^*(\underline{\mathbf{R}}, t) C_k(\underline{\mathbf{R}}, t) \rightarrow \frac{1}{N_{tr}} \sum_I^{N_{tr}} \delta(\underline{\mathbf{R}} - \underline{\mathbf{R}}^{(I)}(t)) C_j^{*(I)}(t) C_k^{(I)}(t) \quad (\text{S.37})$$

and integrating over $\underline{\mathbf{R}}$. The nuclear velocity and the divergence of the current-density become

$$\frac{\mathbf{J}_{\nu}}{|\chi|^2} \Big|_{\underline{\mathbf{R}}=\underline{\mathbf{R}}^{(I)}} = \dot{\mathbf{R}}_{\nu} \Big|_{\underline{\mathbf{R}}=\underline{\mathbf{R}}^{(I)}} \rightarrow \dot{\mathbf{R}}_{\nu}^{(I)} \quad \text{and} \quad \frac{\nabla_{\nu} \cdot \mathbf{J}_{\nu}}{|\chi|^2} \Big|_{\underline{\mathbf{R}}=\underline{\mathbf{R}}^{(I)}} = \partial_t \text{Log}(|\chi|^2) \Big|_{\underline{\mathbf{R}}=\underline{\mathbf{R}}^{(I)}} \rightarrow -2\mathbf{Q}_{\nu}^{(I)} \cdot \dot{\mathbf{R}}_{\nu}^{(I)} \quad (\text{S.38})$$

where we have invoked the equation of continuity. The trajectory's velocity $\dot{\mathbf{R}}_{\nu}^{(I)}$ is given by classical equations of motion derived from the classical nuclear Hamiltonian. Hence, we obtain after integrating Eq. S.33 over $\underline{\mathbf{R}}$

$$\begin{aligned} \partial_t \Gamma_{jk}(t) = & - \sum_I^{N_{tr}} C_j^{(I)*} C_k^{(I)*} \left\{ i\Delta E_{kj}^{(I)} + \sum_{\nu} \left(i\Delta \mathbf{f}_{kj}^{(I)} \cdot \dot{\mathbf{R}}_{\nu}^{(I)} - 2\mathbf{Q}_{\nu}^{(I)} \cdot \dot{\mathbf{R}}_{\nu}^{(I)} - (\mathfrak{S}_{\nu,k}^{(I)} + \mathfrak{S}_{\nu,j}^{(I)}) \cdot \dot{\mathbf{R}}_{\nu}^{(I)} \right) \right. \\ & + \sum_{\nu} \frac{1}{2M_{\nu}} \left[i\Delta \Omega_{\nu,jk}^{(I)} + \sum_l |C_l^{(I)}|^2 (2\mathfrak{Q}_{\nu,j}^{(I)} - \nabla_{\nu}) \cdot \Delta \mathbf{f}_{\nu,lj}^{(I)} + \sum_l |C_l^{(I)}|^2 (2\mathfrak{Q}_{\nu,k}^{(I)} - \nabla_{\nu}) \cdot \Delta \mathbf{f}_{\nu,lk}^{(I)} \right. \\ & \left. \left. + 4 \sum_l |C_l^{(I)}|^2 \mathfrak{S}_{\nu,l}^{(I)} \cdot \mathbf{f}_{\nu,l}^{(I)} + i\mathbf{f}_{\nu,k}^{(I)2} - i\mathbf{f}_{\nu,j}^{(I)2} - 2i\Delta \mathbf{f}_{\nu,kj}^{(I)} \cdot \sum_l |C_l^{(I)}|^2 \mathbf{f}_{\nu,l}^{(I)} \right] \right\} \quad (\text{S.39}) \end{aligned}$$

Further, using the fact that $\overline{\mathfrak{Q}}_{\nu,kj} = \mathbf{Q}_{\nu}^{(I)} - \frac{1}{2}(\mathfrak{S}_{\nu,k}^{(I)} + \mathfrak{S}_{\nu,j}^{(I)})$, we write

$$\begin{aligned} \partial_t \Gamma_{jk}(t) = & - \sum_I^{N_{tr}} C_j^{(I)*} C_k^{(I)*} \left\{ i\Delta E_{kj}^{(I)} + \sum_{\nu} \left(i\Delta \mathbf{f}_{kj}^{(I)} - 2\overline{\mathfrak{Q}}_{\nu,kj} \right) \cdot \dot{\mathbf{R}}_{\nu}^{(I)} + \sum_{\nu} \frac{1}{2M_{\nu}} \left[i\Delta \Omega_{\nu,jk}^{(I)} \right. \right. \\ & + \sum_l |C_l^{(I)}|^2 (2\mathfrak{Q}_{\nu,j}^{(I)} - \nabla_{\nu}) \cdot \Delta \mathbf{f}_{\nu,lj}^{(I)} + \sum_l |C_l^{(I)}|^2 (2\mathfrak{Q}_{\nu,k}^{(I)} - \nabla_{\nu}) \cdot \Delta \mathbf{f}_{\nu,lk}^{(I)} \\ & \left. \left. + 4 \sum_l |C_l^{(I)}|^2 \mathfrak{S}_{\nu,l}^{(I)} \cdot \mathbf{f}_{\nu,l}^{(I)} + i\mathbf{f}_{\nu,k}^{(I)2} - i\mathbf{f}_{\nu,j}^{(I)2} - 2i\Delta \mathbf{f}_{\nu,kj}^{(I)} \cdot \sum_l |C_l^{(I)}|^2 \mathbf{f}_{\nu,l}^{(I)} \right] \right\} \quad (\text{S.40}) \end{aligned}$$

We consider the total time-derivative along the trajectory, defined using the convective derivative (Lagrangian frame) $d/dt = \partial_t + \sum_{\mu} \dot{\mathbf{R}}_{\mu}^{(I)} \cdot \nabla_{\mu}$. This yields:

$$\frac{d\Gamma_{jk}}{dt} \rightarrow \left(\partial_t + \sum_{\nu} \dot{\mathbf{R}}_{\nu} \cdot \nabla_{\nu} \right) \Gamma_{jk} = \partial_t \Gamma_{jk}(t) + \sum_{\nu} \dot{\mathbf{R}}_{\nu} \cdot (i\Delta \mathbf{f}_{\nu,kj} - 2\overline{\mathfrak{Q}}_{\nu,kj}) \Gamma_{jk} \quad (\text{S.41})$$

Eq. (S.40) with (S.41) gives the *exact* equation for the coherences for trajectory-based methods in regions of negligible NAC. Writing in terms of the coefficients (Eq. (S.37)), we obtain

$$\begin{aligned} \sum_I \frac{d(C_j^* C_k)^{(I)}}{dt} &= - \sum_I C_j^{*(I)} C_k^{(I)} \left\{ \sum_{\nu,l} \frac{|C_l|^2}{2M_\nu} \left[\overline{(4\mathcal{Q}_{\nu,jk}^{(I)} - 2\nabla_\nu)} \cdot (\mathbf{f}_{\nu,l}^{(I)} - \mathbf{f}_{\nu,jk}^{(I)}) + 4\mathfrak{S}_{\nu,l}^{(I)} \cdot \mathbf{f}_{\nu,l}^{(I)} \right] \right. \\ &\quad \left. + i\Delta E_{kj}^{(I)} + \sum_\nu \frac{1}{2M_\nu} \left[i\Delta\mathfrak{Q}_{\nu,jk}^{(I)} + i\Delta(\mathbf{f}_{\nu,kj}^{(I)})^2 - 2i\Delta\mathbf{f}_{\nu,kj}^{(I)} \cdot \sum_l |C_l^{(I)}|^2 \mathbf{f}_{\nu,l}^{(I)} \right] \right\} \end{aligned} \quad (\text{S.42})$$

Defining $\widetilde{C_j^* C_k}^{(I)} = C_j^{*(I)*} C_k^{(I)} e^{i \int (\alpha_{jk} - \sum_\nu \frac{\Delta \mathbf{f}_{kj} \cdot \dot{\mathbf{R}}_\nu}{|\chi|^2}) dt}$ we can write

$$\frac{d(\widetilde{C_j^* C_k}^{(I)})}{dt} = - \widetilde{C_j^* C_k}^{(I)} \left\{ \sum_\nu \frac{1}{2M_\nu} \sum_l |C_l^{(I)}|^2 \left[\overline{(4\mathcal{Q}_{\nu,jk}^{(I)} - 2\nabla_\nu)} \cdot (\mathbf{f}_{\nu,l}^{(I)} - \mathbf{f}_{\nu,jk}^{(I)}) + 4\mathfrak{S}_{\nu,l}^{(\alpha)} \cdot \mathbf{f}_{\nu,l}^{(I)} \right] \right\} \quad (\text{S.43})$$

which by the same argument as given below Eq. S.35 the equation holds for $|C_j^* C_k|^{(I)}$, as given in Eq. 10 of the main text.

Finally, to define the exact trajectory-based propagation equations, we now go back and include the terms from the NAC.

$$\partial_t \Gamma_{jk}(\underline{\mathbf{R}}, t) = \partial_t \Gamma_{jk}(\underline{\mathbf{R}}, t)^{\text{Eq. S.33}} + \partial_t \Gamma_{jk}(\underline{\mathbf{R}}, t)^{\text{NAC}} \quad (\text{S.44})$$

where

$$\begin{aligned} \partial_t \Gamma_{jk}(\underline{\mathbf{R}}, t)^{\text{NAC}} &= - \sum_{\nu, n \neq k} \frac{\Gamma_{jn}}{2M_\nu} \left[-iD_{kn,\nu} + 2\mathbf{d}_{kn,\nu} \cdot \left(\frac{M_\nu \mathbf{J}_\nu}{|\chi|^2} + \sum_l |C_l|^2 \Delta \mathbf{f}_{\nu,nl} + i \sum_{ml} C_l^* C_m \mathbf{d}_{\nu,lm} + i \mathcal{Q}_{\nu,n} \right) \right] \\ &+ \sum_{\nu, n \neq j} \frac{\Gamma_{nk}}{2M_\nu} \left[-iD_{nj,\nu} - 2\mathbf{d}_{jn,\nu} \cdot \left(\frac{M_\nu \mathbf{J}_\nu}{|\chi|^2} + \sum_l |C_l|^2 \Delta \mathbf{f}_{\nu,nl} + i \sum_{ml} C_l^* C_m \mathbf{d}_{\nu,lm} - i \mathcal{Q}_{\nu,n} \right) \right] \\ &+ \sum_\nu \frac{\Gamma_{jk}}{2M_\nu} \left[4i \overline{\mathcal{Q}}_{\nu,jk} \cdot \sum_{lm} C_l^* C_m \mathbf{d}_{\nu,lm} + 2 \sum_{lm} (\Delta \mathbf{f}_{\nu,lm} - 2i \overline{\mathfrak{S}}_{\nu,lm} + i \nabla_\nu) \cdot \mathbf{d}_{\nu,lm} - 2\Delta \mathbf{f}_{\nu,jk} \cdot \sum_{lm} C_l^* C_m \mathbf{d}_{\nu,lm} \right] \end{aligned} \quad (\text{S.45})$$

so that for the trajectory-based coherences and populations, we obtain

$$\sum_I \frac{d(C_j^* C_k)^{(I)}}{dt} = \sum_I \left(\frac{dC_j^* C_k^{(I)}}{dt} \right)^{\text{Eq. S.42}} + \left(\frac{dC_j^* C_k^{(I)}}{dt} \right)^{\text{NAC}} \quad (\text{S.46})$$

where

$$\begin{aligned} \left(\frac{dC_j^* C_k^{(I)}}{dt} \right)^{\text{NAC}} &= - \sum_{\nu, n \neq k} \frac{(C_j^* C_n)^{(I)}}{2M_\nu} \left[-iD_{kn,\nu}^{(I)} + 2\mathbf{d}_{kn,\nu}^{(I)} \cdot \left(M_\nu \dot{\mathbf{R}}_\nu^{(I)} + \sum_l |C_l^{(I)}|^2 \Delta \mathbf{f}_{\nu,nl}^{(I)} + i \sum_{ml} (C_l^* C_m)^{(I)} \mathbf{d}_{\nu,lm}^{(I)} \right. \right. \\ &\quad \left. \left. + i \mathcal{Q}_{\nu,n}^{(I)} \right) \right] + \sum_{\nu, n \neq j} \frac{(C_n^* C_k)^{(I)}}{2M_\nu} \left[-iD_{nj,\nu}^{(I)} - 2\mathbf{d}_{jn,\nu}^{(I)} \cdot \left(M_\nu \dot{\mathbf{R}}_\nu^{(I)} + \sum_l |C_l^{(I)}|^2 \Delta \mathbf{f}_{\nu,nl}^{(I)} + i \sum_{ml} (C_l^* C_m)^{(I)} \mathbf{d}_{\nu,lm}^{(I)} - i \mathcal{Q}_{\nu,n}^{(I)} \right) \right] \\ &+ \sum_\nu \frac{(C_j^* C_k)^{(I)}}{M_\nu} \sum_{lm} C_l^{*(I)} C_m^{(I)} \left[2i \overline{\mathcal{Q}}_{\nu,jk}^{(I)} + \Delta \mathbf{f}_{\nu,lm}^{(I)} - 2i \overline{\mathfrak{S}}_{\nu,lm}^{(I)} + i \nabla_\nu + \Delta \mathbf{f}_{\nu,kj}^{(I)} \right] \cdot \mathbf{d}_{\nu,lm}^{(I)} \end{aligned} \quad (\text{S.47})$$

SM.3 SIMULATION DETAILS

For the quantum dynamics (QD) simulations, the time-dependent Schrödinger equation is solved on a grid in the diabatic basis using the split-operator method. The system is initialized in a coherent superposition of three gaussian nuclear wavepackets

$$|\Psi(R, 0)\rangle = \chi(R, 0) (|\phi_{R,1}\rangle + |\phi_{R,2}\rangle/2 + |\phi_{R,3}\rangle/2) \quad (\text{S.48})$$

with $\chi(R, 0) = \left(\frac{2\pi^{1/2}}{3\sigma}\right)^{1/2} e^{-\frac{(R-R_0)^2}{2\sigma^2} + i(R-R_0)P_0}$. The initial variance, position, momentum are $(\sigma, R_0, P_0) = (1 \text{ bohr}, -26 \text{ bohr}^{-1}, 40 \text{ bohr})$ for the EL20-SAC model and $(\sigma, R_0, P_0) = (0.223 \text{ bohr}, -4 \text{ bohr}, 0 \text{ bohr}^{-1})$ for the 3HO model. For the EL20-SAC model the spatial grid is defined in the range $[-26 : 28]$ bohr with 4000 grid points and with a time-step of $dt = 0.0012$ fs. For the 3HO model the chosen spatial grid range is $[-10 : 10]$ bohr with 2000 grid points and with a time-step of $dt = 0.0024$ fs.

The trajectory-based simulations were performed in the G-CTMQC package [52] and the SHXF simulations in the PYUNIXMD package [44]. In both models 1000 Wigner-sampled trajectories were run using the same initial conditions as for the exact case. The initial trajectory ensemble for all methods, was initialized in a pure ensemble, i.e each trajectory carries the same coherent superposition of electronic states. The active states for the surface hopping simulations were stochastically selected to match the net populations at the initial time. We refer the reader to Ref. [10] for a study on different choices (pure and mixed) of initial electronic state in trajectory-based methods.

Example 1: EL20-SAC

The Hamiltonian in the diabatic basis is given by

$$H(R) = \begin{pmatrix} V_1(R) & 0 & 0 \\ 0 & V_2(R) & \lambda(R) \\ 0 & \lambda(R) & -V_2(R) \end{pmatrix} \quad (\text{S.49})$$

with

$$\begin{aligned} V_1(R) &= -0.03(R + 35) - 0.02 \\ V_2(R) &= \frac{R}{|R|} A \left(1 - e^{-B|R|}\right) \\ \lambda(R) &= C e^{-DR^2} \end{aligned} \quad (\text{S.50})$$

the chosen model parameters were $A = 0.01 \text{ Ha}$, $B = 1.6 \text{ bohr}^{-1}$, $C = 0.005 \text{ Ha}$ and $D = 1 \text{ bohr}^{-2}$.

Example 2: 3HO

The Hamiltonian reads

$$H(R) = \begin{pmatrix} \frac{1}{2}k_1R^2 & 0 & 0 \\ 0 & \frac{1}{2}k_2R^2 + \Delta & 0 \\ 0 & 0 & \frac{1}{2}k_2R^2 + 2\Delta \end{pmatrix} \quad (\text{S.51})$$

with $k_1 = 0.005 \text{ Ha}^2$, $k_2 = 0.02 \text{ Ha}^2$ and $\Delta = 0.01 \text{ Ha}$.

SM.4 EFFECT OF \mathfrak{S}

To show the importance of $\mathfrak{S}(R, t)$ we plotted time-snapshots of the exact $Q_1(R, t)$, $\mathfrak{S}_1(R, t)$ and $\mathcal{Q}_1(R, t)$ during the first recoherence event. We observe both the nuclear quantum momentum Q_1 and the reduced contribution \mathfrak{S}_1 are active during this event, and the large features that Q_1 displays are offset largely by \mathfrak{S}_1 yielding a relatively small \mathcal{Q}_1 . As discussed in the main text, the \mathfrak{S} terms are responsible to induce recoherence away from NAC regions causing a change in the electronic coherences which then activates the terms dependent on $Q(R, t)$.

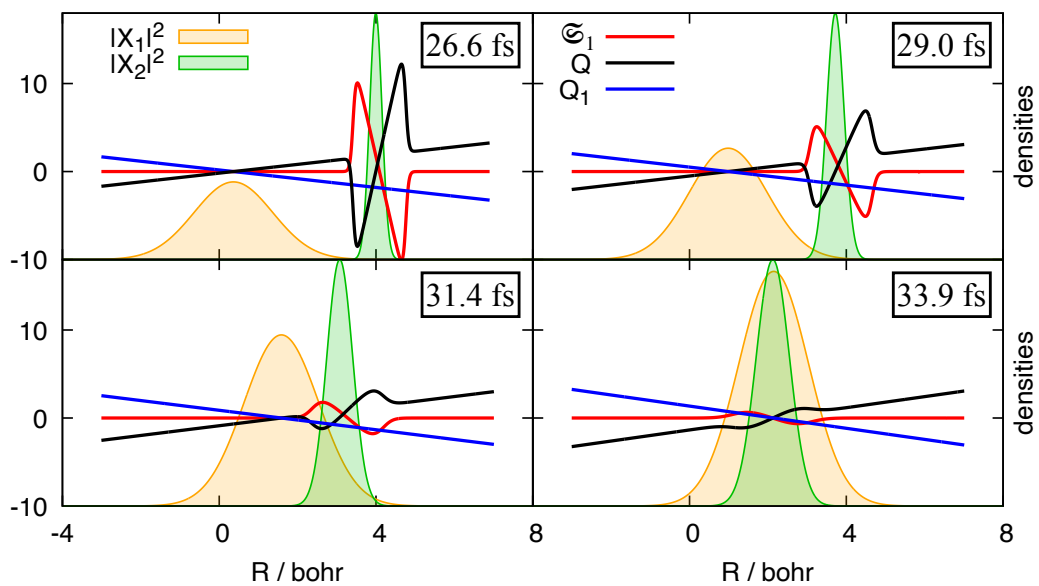


FIG. S.1. Time snapshots of the exact density on the first (orange) and second (green) electronic states, nuclear quantum momentum (blue line), and projected quantum momentum (black line) and crunch term (red line) on state 1 during the recoherence event for 3HO model.